Nafta-Gaz 2025, no. 3, pp. 210–216, DOI: 10.18668/NG.2025.03.07

Overview of calculation techniques of extreme wave loads on stationary offshore oil and gas platforms

Przegląd technik obliczeniowych dotyczących ekstremalnych obciążeń falowych na stacjonarnych morskich platformach ropnych i gazowych

Vahid T. Mustafayev, Chingiz R. Nasirov

Azerbaijan State Oil and Industry University, Azerbaijan

ABSTRACT: Offshore stationary oil and gas platforms are continuously subjected tovarious dynamic loads, including wave, wind, seismic, and equipment-induced forces. Among these, wave loads have the most detrimental effect on the stability of offshore installations. When waves impact the structure, they cause material degradation, vibrations, and other damage to structural elements. Occasionally, offshore structures may be struck by extremely large waves, which can lead to catastrophic consequences. The occurrence of such waves is less predictable than other hazardous natural phenomena, such as hurricanes. Extreme wave loads are considered during the design phase and are typically evaluated using scaled models in special water pools. Various techniques exist for modeling these extreme wave loads, allowing for cost reduction and acceleration of the design process for offshore installations. The article examines different techniques used to calculate velocity distributions in a fluid medium under the influence of giant waves on offshore oil and gas installations. A brief analysis of research on the effects of tsunami waves on barriers (vertical walls and cylinders), idealizing some of the main types of offshore installations, is also presented. Wave loads play a significant role in the Caspian Sea where, based on the operating experience of various offshore oil and gas installations, such wave loads can cause significant damage to different types of platforms. For this reason, correct modeling of various dynamic loads, especially giant waves, during the design stage plays a pivotal role in ensuring safety of personnel and the environment.

Key words: numerical methods, velocity distribution, giant waves, wave height.

STRESZCZENIE: Stacjonarne morskie platformy ropne i gazowe są nieustannie narażone na różne obciążenia dynamiczne, w tym fale, wiatr, wstrząsy sejsmiczne oraz siły generowane przez pracujące urządzenia. Spośród tych czynników to obciążenia falowe mają najbardziej destrukcyjny wpływ na stabilność konstrukcji morskich. Oddziaływanie fal na platformy prowadzi do degradacji materiałów, powstawania wibracji oraz uszkodzeń elementów konstrukcyjnych. Czasami konstrukcje morskie są poddawane uderzeniom ekstremalnie wysokich fal, co może mieć katastrofalne skutki. Występowanie takich fal jest trudniejsze do przewidzenia niż innych zjawisk naturalnych, takich jak huragany. Ekstremalne obciążenia falowe są uwzględniane już na etapie projektowania i zazwyczaj analizowane przy użyciu modeli skalowanych w specjalnych basenach badawczych. Istnieje wiele technik modelowania tych obciążeń, co pozwala na redukcję kosztów oraz przyspieszenie procesu projektowania morskich instalacji. Artykuł omawia różne metody wykorzystywane do obliczania rozkładów prędkości w środowisku wodnym pod wpływem olbrzymich fal działających na morskie platformy naftowe i gazowe. Przedstawiono także krótką analizę badań nad wpływem fal tsunami na bariery (ściany pionowe i cylindry), które symulują niektóre z głównych typów morskich instalacji. Obciążenia falowe odgrywają szczególną rolę na Morzu Kaspijskim, gdzie – na podstawie doświadczeń eksploatacyjnych różnych morskich platform ropnych i gazowych – mogą powodować znaczne uszkodzenia różnych typów konstrukcji. Z tego względu prawidłowe modelowanie różnych obciążeń dynamicznych, w tym zwłaszcza ogromnych fal, na etapie projektowania odgrywa kluczową rolę w zapewnieniu bezpieczeństwa personelu, jak również ze względu ochrony środowiska.

Słowa kluczowe: metody numeryczne, rozkład prędkości, gigantyczne fale, wysokość fali.

Corresponding author: Ch.R. Nasirov, e-mail: *cina-01@mail.ru*

Article contributed to the Editor: 21.11.2023. Approved for publication: 05.03.2025.

Introduction

Stationary offshore oil and gas installations, such as platforms, can be located at a depth of up to 100 meters in regions subject to significant wave and wind loads. Examples include "Absheron" platform on the Caspian Sea shelf (State Website of SOCAR) and the "Hebron" platform on the Canadian shelf near the Newfoundland Peninsula (Widianto et al., 2013).

Offshore stationary oil platforms are designed based on individual project requirements; however, many share common structural elements. Typically, they have an underwater base (either cylindrical or parallelepiped) situated on the seabed. Some designs incorporate a caisson, on which one or more columns are positioned. The primary production operations take place on the topside, which accommodates various facilities such as a drilling rig, residential module, helipad, etc. An example of a caisson-based platform design was presented by Widianto et al. (2013).

During operation, a large number of personnel are present on-site. Therefore, offshore platforms must be designed to withstand various loads, including those from natural forces, prevent disastrous situations (Hauguel, 2010).

Furthermore, certain platforms that are not connected by oil pipelines to onshore facilities incorporate storage capacity for large volumes of produced oil (exceeding 1 million barrels) (Widianto et al., 2013). In the event of structural failure, a breach in oil containment could result in a significant spill, causing severe environmental damage.

Due to aforementioned reasons, the design of offshore platforms must be conducted with high precision. When designing stationary offshore structures, statistical data on the frequency of giant wave occurrences is utilized. As a rule, model tests of hydraulic structures are carried out in special basin to determine wave loads (Amaziah, 2011).

Numerical methods for solving the Navier-Stokes equations were developed for use in problems involving wave impact calculations on ships (the "green water effect") to enhance navigation safety (Sheng et al., 2011), where floating oil platforms were also considered. An oncoming wave collides with the structure and then breaks against a column. Behind the column, the water streams flowing around it collide, forming a water column, the so-called "rooster tail". Such a release of water, in the event of a giant wave impact, can strongly affect the upper structure from below (Gudmestad, 2020) and pose a threat to the platform. In model tests, the rooster tail effect is recreated, but a detailed flow pattern is not presented (Pagliara et al., 2011). Due to the significant risk posed by giant waves, their modeling and calculation are of great importance for ensuring the safety of fixed offshore platforms. The following sections consider the main aspects of offshore structures calculations related to wave loads, specifically the impact of tsunami waves on the full profile of the structure and on vertical barriers with a large cross-section. Additionally, an example of wave impact calculations is presented.

Wave parameters

The parameters of giant waves, such as wave height and wave period, are described as probability distributions over observation intervals of 1, 10, 100 and 1000 years. Over an annual period, the most probable wave has a height of 10.5 m and a period of 13 seconds. For a 100-year period, a wave with a height of 15 m and a period of 16 seconds is more likely to occur, for example, in the North Sea (Oberlies et al., 2014). In the Caspian Sea, the maximum height of giant waves can reach 10–11.7 m, with a period of 10–11 seconds (Myslenkova et al., 2018). Such wave heights correspond to the initial values of the velocities of water rise from the lowest point of the wave to the crest on the order of 14–17 m/s.

According to the theory describing waves in a fluid in a gravitational field (Apel, 1986), the maximum horizontal wave velocity vx in a shallow water body is given by:

$$v_x = \sqrt{gh} \qquad (1)$$

where:
g – free-fall acceleration,
h – depth of the water body.

The horizontal velocity is much greater than the vertical velocity when considering wave motion with a horizontal component. The dependence of the velocity V on time t and depth distribution is presented in the following form:

$$V(x,z,t) = V_0 \cosh\big(k(z+h)\big)\sin(kx-\omega t) \qquad (2)$$

where:
V_0 – amplitude of the wave,
z – depth (z equal to $-h$ corresponds to the bottom of the water body),
x – coordinate along the surface of the water body,
k – wave number,
ω – frequency,
t – time,
cosh – hyperbolic cosine.

Impact of tsunami waves on full-profile structures

Large-scale numerical studies of tsunami wave propagation (based on finite-difference models) in both model and real-world areas of the World Ocean, as well as studies on tsunami wave runup onshore, have been conducted by various authors (Marchuk et al., 1983; Shokin et al., 1989).

A comprehensive review of currently used analytical models for tsunami wave formation, propagation across sea area, transformation in the coastal zone, and runup on a sloping shore is presented in the monograph (Bandyopadhyay et al., 2021).

Various studies have produced different results regarding the interaction of long waves with impermeable barriers of full profile in classical problems where the barrier is a vertical wall. In particular, Harlow and Wetch (1965) evaluated the impact of a solitary wave based on the numerical solution of the Navier-Stokes equations using the finite-difference method of markers on a grid.

Asymptotic expansions of different orders (Su and Gardner, 1969) were applied to solve the same problem in a nonlinear formulation for an ideal fluid. A numerical solution based on the Fourier transform method in coordinates and finite-difference scheme in time was obtained by Fenton and Reincker (1982). The application of Riemann invariants made it possible to derive simple relations for calculating the height of a long wave on a wall (Pelinovsky et al., 2008). The main features of the interaction between solitary waves and a vertical wall are satisfactorily described by numerical solutions of long-wave nonlinear dispersive equations that are not limited by the smallness condition of the wave amplitude (Haugel, 2010; Zhou et al., 1991). Zheleznyak (1985), based on the numerical solution of the nonlinear dispersion approximation of long-wave equations, estimated the distribution of force characteristics at liquid depth. The variation of the free surface profile $\eta(x, t)$ and the average particle velocity $u(x, t)$ over depth is described by the following equations (Zheleznyak, 1985):

$$
\begin{gathered}
(hu)_t + \left(hu^2 + \frac{gh^2}{2} - \frac{h^3}{3} R - \frac{h^2}{3} Q \right) = \\
= d_x \left(gh - \frac{h^2}{2} R - hQ \right) - c_f u|u| \\
h_t + (hu)_x = 0
\end{gathered} \tag{3}
$$

where: $R = u_{xt} + u \cdot u_{xx} - u_x^2$; $Q = (u_t + u \cdot u_x) d_x + u^2 d_{xx}$ – fluid flow rate; $h = d + \eta$; d depth of the fluid; c_f – bottom friction coefficient; u_x – partial derivative of u; u_{xt} – mixed partial derivative of u with respect to both spatial parameter x and time t; u_{xx} – second partial derivative of u with respect to t; d_x – partial derivative of the fluid depth with respect to x; d_{xx} – second partial derivative of the fluid depth with respect to x.

The boundary conditions on the wall are derived from the conditions of impermeability and symmetry of motion (Zheleznyak, 1985):

$$
u = 0,\ \eta_x = 0,\ u_{xx} = 0,\ x = L \tag{4}
$$

When analyzing the impact of an individual wave pulse on a wall, the parameters of the incoming wave are defined by the initial conditions for the functions h and u over the segment $x_0 - \lambda_0/2 \le x \le x_0 + \lambda_0/2$, where x_0 – coordinate of maximum wave elevation; λ_0 – characteristic wavelength (determined from the relation $\eta(x_0 \pm \lambda_0/2) = 10^{-3} a$ (a – initial amplitude of the wave; η – surface elevation of the wave).

If a is the initial amplitude in the remaining part of the computational domain, it must be assumed that $\eta = u = 0$. At the input boundary ($x = 0$), free wave conditions are set, and the initial perturbation is represented by a single wave (Zheleznyak, 1985):

$$
\begin{gathered}
\frac{h(0,x)}{d_0} = 1 + a \cdot ch^{-2} \left[\sqrt{\frac{3\alpha}{4(1+\alpha)}} \cdot \frac{x - x_0}{d_0} \right], \\
u(0,x) = \frac{\eta}{h} \sqrt{g d_0 (1+\alpha)}
\end{gathered} \tag{5}
$$

or as a sinusoidal pulse:

$$
\begin{gathered}
\frac{h(0,x)}{d_0} = 1 + a \cdot \sin \frac{\pi}{\lambda_0} \left(x - x_0 + \frac{\lambda_0}{2} \right), \\
u(0,x) = 2\sqrt{gh} - \sqrt{g d_0}
\end{gathered} \tag{6}
$$

where:

α – relative initial wave amplitude,

d_0 – initial depth at $x = x_0$.

The total pressure depth distribution is determined by the formula:

$$
\frac{p}{\rho g d} = \frac{\eta - z}{d} - \frac{1}{2} \left[\left(\frac{h}{d} \right)^2 - \left(\frac{z}{d} + 1 \right)^2 \right] \frac{Rd}{g} - \frac{\eta - z}{d} \frac{Q}{g} \tag{7}
$$

Where the z-axis is directed vertically upwards from the undisturbed free surface level.

The dynamic component of pressure is determined depending on the value of z:

$$
p_* = \begin{cases} p, & z \ge 0 \\ p + \rho g z, & z < 0 \end{cases} \tag{8}
$$

The hydrodynamic force acting on a vertical wall is expressed as:

$$
\frac{F}{\rho g d^2} = \frac{1}{\rho g d^2} \int_{-d}^{\eta} p_* dz = \frac{1}{2} \left[\left(\frac{h}{d} \right)^2 - 1 \right] - \frac{1}{3} \left(\frac{h}{d} \right)^3 \frac{Rd}{g} \tag{9}
$$

and the overturning moment relative to its base as:

$$
\frac{M}{\rho g d^3} = \frac{1}{\rho g d^3} \int_{0}^{\eta} p_* z' dz' = \frac{1}{6} \left[\left(\frac{h}{d} \right)^3 - 1 \right] - \frac{1}{8} \left(\frac{h}{d} \right)^4 \frac{Rd}{g} \tag{10}
$$

where: $z' = z + d$; $Q = 0$.

The formulated initial boundary value problem is solved using a three-layer finite-difference predictor-corrector scheme. The analytical solution for standing waves was obtained by Newman (1974).

The free surface elevation and pressure were compared to evaluate the obtained results of the problem solution of long waves interaction with a vertical wall.

Calculations were performed using analytical expressions considering the linear theory of shallow water waves (Karmakar, 2019):

$$\frac{\eta_m}{d} = 2a \tag{11}$$

second-order solitary wave theory (Gear and Grimshaw, 1983):

$$\frac{\eta_m}{d} = 2a + \frac{\alpha^2}{2} \tag{12}$$

non-linear shallow water theory (Gear and Grimshaw, 1983):

$$\frac{\eta_m}{d} = 4(1 + \alpha - \sqrt{1+\alpha}) \tag{13}$$

and using numerical methods (Zheleznyak, 1985),
where:

η_m – maximum of the free surface elevation on the vertical wall
a – wave amplitude
$\alpha = a/d_0$ – relative wave amplitude.

The results of the hydrodynamic force and moment calculations are in full agreement with the data of Fenton and Reincker (1982) for $\alpha \leq 0.4$. For $\alpha \geq 0.5$ a loss of accuracy in calculations is noted. At the same time, the results of calculations performed by Wuppukondur and Baldock (2022) agree satisfactorily with the experimental data obtained by Jensen

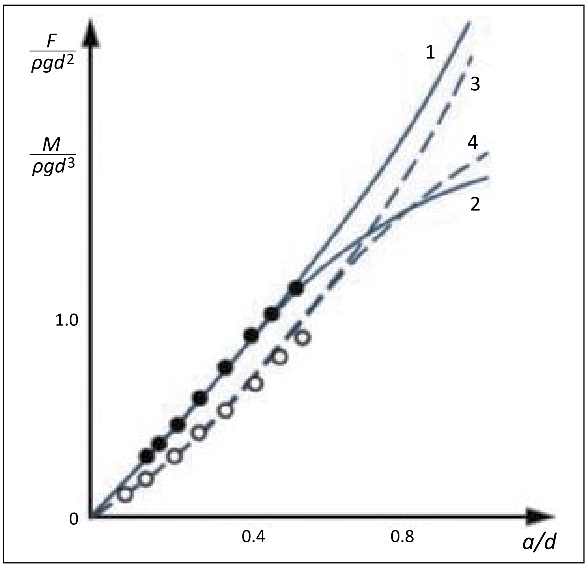

Figure 1. Values of force and overturning moment as a function of relative wave amplitude: 1 and 3 – maximum values of force and moment; 2 and 4 refer to the moment of time when the maximum splash occurs (Fenton and Reincker, 1982)

Rysunek 1. Wartości siły i momentu wywracającego w funkcji względnej amplitudy fali: 1 i 3 – maksymalne wartości siły i momentu; 2 i 4 odnoszą się do momentu, w którym występuje maksymalny rozbryzg (Fenton i Reincker, 1982).

(2019), even for values of α exceeding the threshold value of 0.8, which approximately corresponds to the onset of solitary wave collapse.

The results of calculating the maximum values of force and moment using Equations (3)–(4) in the range of relative amplitude $0 \leq \alpha \leq 0.8$ are approximated by cubic polynomials:

$$\begin{aligned} \bar{F} &= 2.26\alpha - 0.602\alpha^2 + 0.820\alpha^3; \\ \bar{M} &= 1.29\alpha + 0.690\alpha^2 + 0.352\alpha^3 \end{aligned} \tag{14}$$

The values of the force acting on the vertical wall and the overturning moment as a function of the relative amplitude of the wave a/d are presented in Figure 1. Light and dark circles (3 and 4) represent calculation data obtained by Fenton and Reincker (1982).

Wave action on a vertical barrier of large cross-section

A key characteristic of the considered case is that the length of a single wave tends to infinity, while the parameter $kD/2$, (k – wave number; D – obstacle diameter), which determines the applicability of diffraction theory, tends to zero. In this case, another parameter is introduced to estimate the flow regime. Considering that the effective wavelength (the segment of the wavelength containing most of the kinetic energy) is proportional to $\sqrt{d^3/h}$, we estimate the parameter $\sqrt{ha^2/d^3}$. According to Isaacson (1983), diffraction theory is applicable to problems involving the interaction of a solitary wave with obstacles when $\sqrt{ha^2/d^3} \geq 0.36$ and when $ka > 0.2\pi$.

Isaacson (1983) presented results based on numerical methods, with approximate solutions for the effect of a solitary wave on a vertical cylinder.

Additionally, the problem of long-wave diffraction on a vertical cylinder is considered in cylindrical coordinate system and is reduced to solving the wave equation:

$$\Delta\psi - \psi_{tt} = 0 \tag{15}$$

boundary conditions:

$$\partial/\partial r(\chi + \psi) = 0,\ r = a;\ \psi \to 0,\ r \to \infty \tag{16}$$

where:

ψ – desired function describing the diffraction field,
χ – function specifying the incident wave,
r – radius-vector of the point.

The methods covered in this study include both theoretical and experimental analyses of tsunami waves impact on key types of offshore oil and gas structures, specifically vertical wall and vertical cylindrical streamlined obstacles.

Example of numerical modeling problem

The modeling was conducted using MATLAB software. The horizontal impulse of the wave is converted into a vertical one upon entering shallow water. A wave with an amplitude of 5 m/s (corresponding to a maximum wave speed of 10 m/s at the sea surface) and a period of 16 s was chosen for modeling, consistent with the probability distributions of wave height and period.

In this example, the motion of a medium is simulated when a wave impacts a stationary offshore structure using numerical methods. The structure used in the calculations is shown in Figure 4. It is positioned at the seabed and consists of a base platform in the shape of a parallelepiped with a height of 20 m and length of 80 m. A column with a diameter of 40 m and a height of 60 m is located on top of the platform. The sea level, represented by a black line, is at a height of 40 m from the lower edge of the parallelepiped (Figure 2). A wave with a maximum horizontal velocity of 10 m/s and a period of 16 s strikes the structure. The velocity distribution over depth corresponds to distribution (Equation 2).

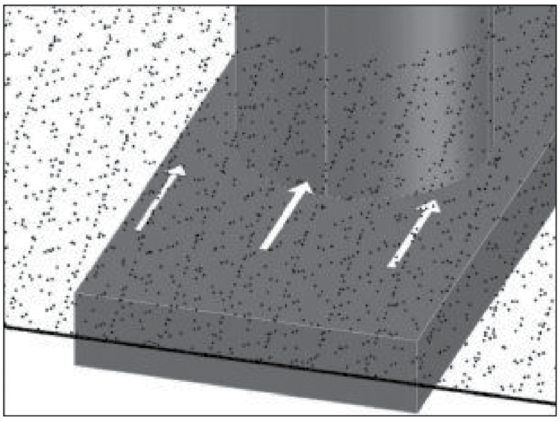

Figure 2. Model of the structure, arrows show the direction of the incoming water flow

Rysunek 2. Model konstrukcji, strzałki wskazują kierunek napływającej wody

The parameters of the medium were calculated within the framework of solving three-dimensional equations of fluid dynamics. When a wave hits the platform of the structure base, it acquires an impulse in the vertical direction, which causes the development of a crest. The initial time of the problem is chosen so that the wave amplitude is maximum at the initial time. The base is at a distance of 2.5 m from the left boundary of the computational domain, which can affect the flow pattern.

The wave load on the structure is determined by the momentum transfer of the fluid; therefore, the velocity distributions are of primary interest. An example of velocity distributions in the horizontal v_x and vertical v_z directions at a time point 0.8 s from the initial time is shown in Figure 3. The distance 0 m corresponds to the left boundary of the computational domain.

The oncoming flow velocity at the left boundary of the computational domain is approximately 10 m/s. The presented distributions were obtained for the near-surface water layer in the middle section of the structure in the direction of the oncoming flow—along the middle arrow in Figure 2. The geometric dimensions of the structure —the base platform and the supporting column in this section—are shown in Figure 4.

By 0.8 s, when interacting with the base of the oil platform, the wave near the sea surface has a vertical velocity component of approximately 5.9 m/s, which is close to the value of the initial horizontal velocity at the bottom of the sea. At the base is located, the wave slows down and its momentum is transformed. The oncoming wave has not yet reached the carrier column, which is located at a distance of 24 m from the left boundary of the computational domain (Figure 2).

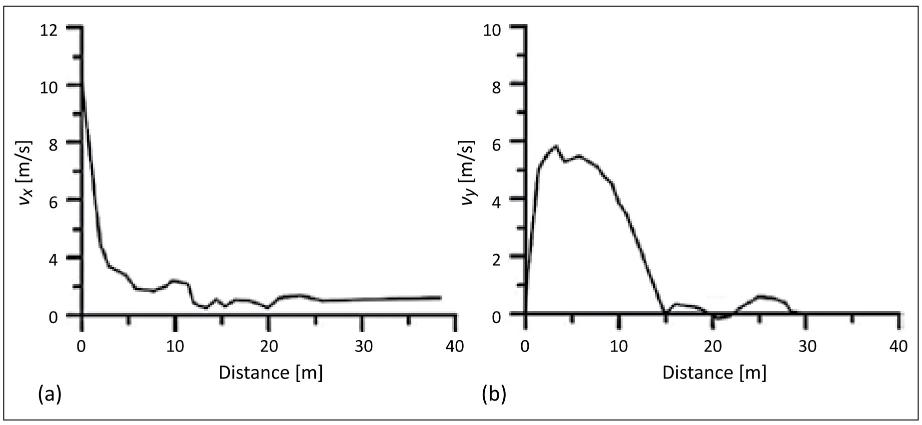

Figure 3. Distributions of horizontal velocity v_x (a) and vertical velocity v_z (b) in the near-surface water layer at a level of 38 m from the sea bottom in the middle section of the structure in the direction of the oncoming flow, at time 0.8 s from the initial time

Rysunek 3. Rozkłady prędkości poziomej v_x (a) i pionowej v_z (b) w przypowierzchniowej warstwie wody na poziomie 38 m od dna morskiego w środkowej części konstrukcji w kierunku napływającego strumienia, w czasie 0,8 s od czasu początkowego

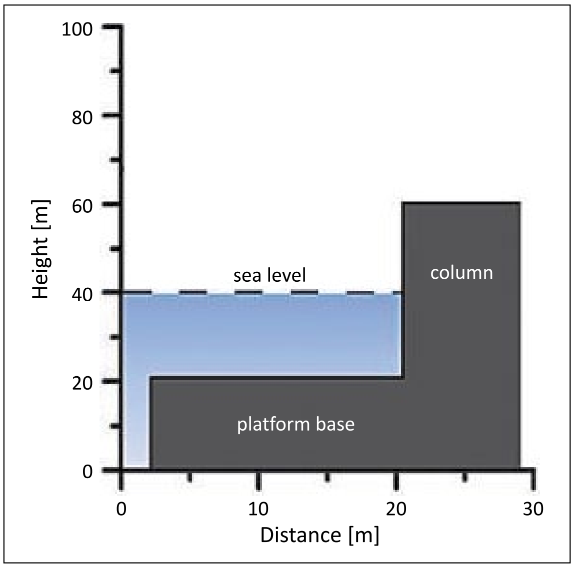

Figure 4. Geometrical dimensions in the section in the middle of the structure along the incoming flow. Zero on the *y*-axis corresponds to the sea bottom, zero on the *x*-axis corresponds to the left input boundary of the computational domain.

Rysunek 4. Wymiary geometryczne w przekroju w środkowej części konstrukcji wzdłuż napływającego strumienia. Zero na osi *y* odpowiada dnu morskiemu, zero na osi *x* odpowiada lewej granicy wejściowej obszaru obliczeniowego.

In the design of oil rigs, full-scale simulation of loads in the basin is used to determine the loads on structural elements, similar to what was done for the Hebron platform (Oberlies et al., 2014). It is believed that analytical methods are not yet "mature enough" for engineering design. However, the method for determining wave loads by testing model structures in the pool has its limitations associated with the number of load cells, their area, the presence of measurement noise, and so on. Another simulation of wave loads was conducted for DolWin Beta platform, the CFD model of which was set up in ComFLOW (Sonneville et al., 2015). The successful simulation conducted by BP for the ACE (Azeri Central East Project Environmental & Social Impact Assessment BP, 2019) platform, using a variety of metaocean data sources, predicted that extreme wave maximum wave heights would range from 9.4–9.6 m and can also be considered as an example (Azeri Central East Project Environmental & Social Impact Assessment BP, 2019).

The advantage of numerical calculations is that they allow results to be obtained faster and at a lower cost than full-scale simulations. Additionally, numerical calculations provide more complete information on loads, as they are not limited by the number or placement of sensors or by data interpretation.

It would be possible to link the results of numerical calculations to a specific oil-producing platform if numerical simulation of model experiments in the basin were performed and the measured loads were compared with the calculated ones.

Conclusion

In conclusion, the overview of various techniques used to calculate the impact of giant waves on stationary offshore installations demonstrates a diversity of approaches, each considering specific conditions. The design characteristics of these installations result in complex interactions with large waves, which must be considered in the design process to prevent catastrophic consequences.

Accurate hydrodynamic modeling, incorporating nonlinear effects and various wave scenarios, forms the foundation for reliable predictions. Overall, a combination of both preliminary simulations and basin experiments will allow for more accurate results, thereby increasing safety of offshore stationary platforms.

References

Amaziah W.O., 2011. Design of Offshore Concrete Gravity Platforms. *Nigerian Journal of Technology*, 30(1): 34–46. DOI: 10.4314/njt.301.49.

Apel J.R., 1986. Linear Response Theory for Waves in a Geophysical Fluid. *Johns Hopkins APL Technical Digest*, 7(1): 42–57.

Azeri Central East Project Environmental & Social Impact Assessment. BP, January 2019.

Bandyopadhyay A., Manna S., Maji D., 2021. Hydrodynamic aspects of tsunami wave motion: a review. *Ocean Dynamics*, 71(5): 613–629. DOI: 10.1007/s10236-021-01454-z.

Fenton J.D., Reincker M.M., 1982. A Fourier method for solving nonlinear water wave problems: application to solitary wave interaction. *Journal of Fluid Mechanics*, 118: 411–443.

Gear J.A., Grimshaw R., 1983. A second order theory for solitary waves in shallow fluids. *Physics of Fluids*, 26 (1): 14–29. DOI: 10.1063/1.863994.

Gudmestad O.T., 2020. Modelling of Waves for the Design of Offshore Structures. *Journal of Marine Sciences and Engineering*, 8(4): 293–301. DOI: 10.3390/jmse8040293.

Harlow F.H., Welch J.E., 1965. Numerical calculation of time-dependent viscous incompressible flow of fluid with free surfaces. *Physics of Fluids*, 8: 2182–2189.

Hauguel A., 2010. A numerical model of storm waves in shallow water. *Environmental Science, Engineering*. DOI: 10.1061/9780872622647.046.

Isaacson M. de St. Q., 1983. Solitary Wave Diffraction around Large Cylinder. *Journal of Waterways, Port, Coastal and Ocean Division*, 109(1): 121–127. DOI: 10.1061/(ASCE)0733-950X(1983)109:1(121).

Jensen A., 2019. Solitary wave impact on a vertical wall. European *Journal of Mechanics – B/Fluids*, 73: 69–74. DOI: 10.1016/j.euromechflu.2018.05.004.

Karmakar T.K., 2019. Wave Propagation and Shallow Water Theory. *Thesis for: Master of Science*.

Marchuk A.G., Chubarov L.B., Shokin Y.I., 1983. Numerical modeling of tsunami waves. *Nauka Press, Siberian Branch, Novosibirsk*, 282.

Myslenkova S.A., Arkhipkina V.S., Pavlova A.V., Dobrolyubova S.A., 2018. Wave Climate in the Caspian Sea Based on Wave Hindcast. *Russian Meteorology and Hydrology*, 43(10): 670–678. DOI: 10.3103/S1068373918100060.

Newman J., 1974. Interaction of water waves with two closely spaced vertical obstacles. *Journal of Fluid Mechanics*, 66(1): 97–106. DOI: 10.1017/S0022112074000085.

Oberlies R., Khalifa J., Huang J., Hetland S., Younan A., Overstake M., Slocum S., 2014. Determination of wave impact loads for the Hebron gravity based structure (GBS). *33rd International Conference on Ocean, Offshore and Arctic Engineering OMAE 2014, June 8–13, San Francisco, California, USA*. OMAE2014-23503. DOI: 10.1115/OMAE2014-23503.

Pagliara S., Kurdistani S. M., Thendiyath R., 2011. Rooster Tail Wave Hydraulics of Chutes, January. *Journal of Hydraulic Engineering*, 137(9): 1085–1088. DOI: 10.1061/(ASCE)HY.1943-7900.0000397.

Pelinovsky E., Kharif C., Talipova T., 2008. Large-amplitude long wave interaction with a vertical wall. *European Journal of Mechanics – B/Fluids*, 27(4): 409–418. DOI: 10.1016/j.euromechflu.2007.08.003.

Sheng S.Ji, Ouahsine A., Smaoui H., Sergent P., 2011, Numerical Prediction of Ship-Generated Waves in Restricted Channel. *International Conference on Computational Methods in Marine Engineering MARINE 2011*.

Shokin Y.I., Chubarov L.B., Marchuk A.G., Simonov K.V., 1989, Computational experiment in the tsunami problem. *Science. Sib. Department. Novosibirsk*.

Sonneville B., Hofland B., Mowinckel A., Paulsen B.T., 2015. Wave Impact Loads on Offshore Gravity Based Structure. *34th International Conference on Ocean, Offshore and Arctic Engineering, OMAE34, May 31–June 5, St. John's, NL, Canada*. DOI: 10.1115/OMAE2015-41879.

State Website of SOCAR. <https://www.socar.az/en/page/absheron> (access: September 2024).

Su G.H., Gardner C.S., 1969. Korteweg-De Vries Equation and Generalizations. 3. Derivation of Korteweg-De Vries Equation and Burgers Equation. *Journal of Mathematical Physics*, 10(3): 536–539. DOI: 10.1063/1.1664873.

Widianto W., Khalifa J., Younan A., Karlsson T., Stuckey P., Gjorven A., 2013. Design of Hebron Gravity Based Structure for Iceberg Impact. *Proceedings of the Twenty-third International Offshore and Polar Engineering, Anchorage, Alaska, June 30–July 5*, 1127–1134.

Wuppukondur A., Baldock T.E., 2022. Physical and numerical modelling of representative tsunami waves propagating and overtopping in converging channels. *Coastal Engineering*, 174: 104120. DOI: 10.1016/j.coastaleng.2022.104120.

Zheleznyak M.I., 1985. The impact of long waves on solid vertical obstacles. In the collection: Rolling waves of tsunami onto the shore. Institute of Appl. *Physicists of the USSR Academy of Sciences. Gorky*, 122–139.

Zhou D., Chan E.S., Melville W.K., 1991. Wave impact pressures on vertical cylinders. *Applied Ocean Research*, 13(5): 220–234. DOI: 10.1016/S0141-1187(05)80046-X.

Vahid Tofig MUSTAFAYEV, Sc.D.
Associate Professor at the Department of Oil and Gas Transportation and Storage
Azerbaijan State Oil and Industry University
16/21 Azadliq Ave., AZ1010 Baku, Azerbaijan
E-mail: *mustafayev.vaqit@mail.ru*

Chingiz Rahim NASIROV, M.Sc.
Ph.D. Student at the Department of Oil and Gas Transportation and Storage
Azerbaijan State Oil and Industry University
16/21 Azadliq Ave., AZ1010 Baku, Azerbaijan
E-mail: *cina-01@mail.ru*